Frontiers of Information Technology & Electronic Engineering
www.jzus.zju.edu.cn; engineering.cae.cn; www.springerlink.com
ISSN 2095-9184 (print); ISSN 2095-9230 (online)
E-mail: jzus@zju.edu.cn

Energy efficiency optimization for a RIS-assisted multi-cell communication system based on a practical RIS power consumption model*

Danning XU, Yu HAN, Xiao LI‡, Jinghe WANG, Shi JIN

National Mobile Communications Research Laboratory, Southeast University, Nanjing 210096, China

E-mail: 220210746@seu.edu.cn; hanyu@seu.edu.cn; li_xiao@seu.edu.cn; wangjh@seu.edu.cn; jinshi@seu.edu.cn

Received Mar. 1, 2023; Revision accepted Sept. 18, 2023; Crosschecked Nov. 8, 2023

Abstract: Reconfigurable intelligent surface (RIS) is widely accepted as a potential technology to assist in communication between base stations (BSs) and users in edge areas. We study the energy efficiency of a RIS-assisted multi-cell communication system with a realistic RIS power consumption model. With the goal of maximizing the energy efficiency of the system, we optimize the transmit beamforming vectors at the BS and the RIS phase shift matrix by a proposed alternative optimization algorithm. First, the transmit beamforming vector is optimized by solving the transformed weighted minimum mean square error (WMMSE) problem. Subsequently, to solve the inconvenience incurred by the discrete relationship between the RIS reflecting unit power consumption and its discrete phase shift, we use a continuous function to approximate their relationship. With this approximation, we can use the majorization minimization (MM) technique to optimize the continuous RIS phase shifts, and then quantize the obtained phase shifts to discrete ones. Simulation results demonstrate that the energy efficiency of the system is effectively optimized by the proposed algorithm.

Key words: Reconfigurable intelligent surface (RIS); Energy efficiency; Multi-cell communication system
https://doi.org/10.1631/FITEE.2300136 **CLC number:** TN929.5

1 Introduction

In the past few decades, benefiting from various technological advancements, fifth-generation wireless communication systems (5G) have achieved high data rates, large system capacity, and low latency. However, high hardware costs and increased energy consumption are still key unresolved issues. Therefore, people look forward to sixth-generation wireless communication systems (6G), and raise higher performance requirements, such as ultra-high data rates, ultra-low latency, ultra-high reliability, and large-scale connection. To meet these demands, various technologies have been proposed by academic and industrial communities. Among them, the reconfigurable intelligent surface (RIS) is a new technology that can intelligently control the wireless transmission environment, and has been recongnized as one of the most promising technologies (Cui et al., 2014, 2017; Tang et al., 2019, 2020).

Generally speaking, RIS is a metasurface composed of many low-cost passive reflecting units, each capable of independently modulating the amplitude and/or phase of the incident signal (di Renzo et al., 2020). The wireless propagation environment becomes controllable by deploying a RIS between transmitters and receivers, and the RIS can lead to better performance, such as higher received signal power,

‡ Corresponding author

* Project supported by the National Natural Science Foundation of China (Nos. 62231009 and 61971126), the Natural Science Foundation of Jiangsu Province, China (No. BK20211511), and the Jiangsu Province Frontier Leading Technology Basic Research Project, China (No. BK20212002)

ORCID: Danning XU, https://orcid.org/0009-0008-9989-3342; Xiao LI, https://orcid.org/0000-0001-9660-9053

better coverage, and lower interference, through proper design. In addition, the RIS has the advantages of light weight, easy installation, and high flexibility. These advantages make the application of the RIS in wireless communication systems very promising (Sang et al., 2022, 2023).

There have been various research activities in the literature recently, involving different aspects of RIS application, such as channel modeling and measurement (Tang et al., 2021), channel estimation (You CS et al., 2021; Huang YW et al., 2022), security communication (Feng et al., 2021b), and artificial intelligent (AI) based design (Feng et al., 2020). Feng et al. (2021a) studied a RIS-assisted orthogonal frequency division multiplexing (OFDM) system. Luo et al. (2021) concentrated on a RIS-assisted multi-cell downlink multi-input single-output (MISO) system with statistical channel state information. Jiang et al. (2023) investigated a user scheduling design in the RIS-assisted communication system. These works proposed effective algorithms to maximize the achievable rate (Gan et al., 2021, 2022; Huang CW et al., 2021).

Energy efficiency is also an important aspect of investigation for RIS-assisted communication systems because green communication is one of the key demands for 6G. The energy efficiency of the RIS-assisted coordinated multi-point (CoMP) system was studied in Chen et al. (2022), where user equipment (UE) association, power allocation, and reflection coefficients were jointly optimized. For non-orthogonal multiple access (NOMA) networks, Wang TQ et al. (2022) investigated the transmit beamforming vectors and RIS phase shift design algorithm to maximize energy efficiency. Liu et al. (2020) studied the energy efficiency of a RIS-assisted simultaneous wireless information and power transfer (SWIPT) network. In the above research, the energy efficiency in different systems was improved through proper RIS design. Nevertheless, almost all of the existing works are based on hypothetical RIS power consumption models, which have not been verified through measurement. The RIS power consumption is assumed to be a constant or even 0 in most existing works, and is independent of the phase shift value of each RIS reflecting unit. Recently, practical measurements of RIS power consumption have been done in Wang JH et al. (2022), where it was shown that the practical RIS power consumption is closely related to the control circuit, the bit resolution of the RIS reflecting units, the polarization direction, and the encoding state of RIS reflecting units.

Thus, we study the RIS-assisted multi-cell downlink transmission system, and try to maximize its energy efficiency based on the practical RIS power consumption model proposed in Wang JH et al. (2022). Different from the model adopted in most existing works, in this model, the RIS power consumption is related to the phase shift values of its reflecting units. To jointly optimize the transmit beamforming vectors at each base station (BS) and the RIS phase shift matrix, we propose an alternative optimization algorithm. First, the weighted minimum mean square error (WMMSE) transformation is performed on the original problem, and we optimize the transmit beamforming vector based on the transformed problem. Then, we establish a continuous function to approximate the discrete relationship between RIS power consumption and phase shift. Finally, we use the majorization minimization (MM) algorithm to optimize the continuous phase shift and discretize it. Numerical results indicate that the proposed algorithm can effectively optimize the energy efficiency of the system.

Notations: $\mathbb{E}\{\cdot\}$ denotes statistical expectation operation; $\mathrm{tr}(\cdot)$ is the trace operation; $\mathrm{Re}(\cdot)$ denotes the real part of a complex number; $\|a\|$ and $|a|$ indicate the norm and the absolute value of a, respectively; $\odot$ represents Hadamard product; the symbols $\{\cdot\}^*$, $\{\cdot\}^{-1}$, $\{\cdot\}^{\mathrm{T}}$, and $\{\cdot\}^{\mathrm{H}}$ represent the conjugate, inverse, transpose, and conjugate transpose operations, respectively; $\mathrm{CN}(\mu,\sigma^2)$ denotes the complex Gaussian distribution with mean μ and variance σ^2; $\mathrm{diag}(\cdot)$ denotes a diagonal matrix with the elements in the brace as its diagonal elements.

2 System model

We consider a RIS-assisted multi-cell downlink communication system in Fig. 1. It contains J cells, each of which deploys a BS with M antennas. There are K single-antenna users in each cell. A single RIS with $N = N_{\mathrm{h}} \times N_{\mathrm{v}}$ reflecting units, arranged in a uniform planar array (UPA) of N_{h} columns and N_{v} rows, is deployed at the edge of adjacent cells. We define $\mathcal{N} \triangleq \{1,2,\cdots,N\}$, $\mathcal{K} \triangleq \{1,2,\cdots,K\}$, and $\mathcal{J} \triangleq \{1,2,\cdots,J\}$ as the sets of RIS reflecting units, users, and cells, respectively.

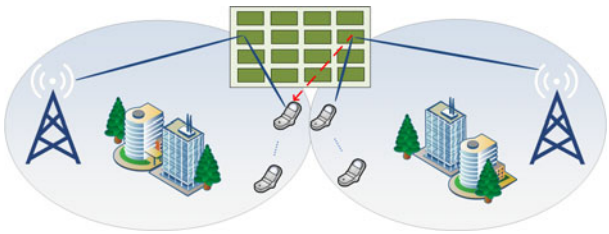

Fig. 1 RIS-assisted multi-cell communication system

2.1 Signal model

The direct path between the BSs and considered users covered by the RIS in each cell is assumed to be blocked by obstacles, or else very weak compared to the reflected path through the RIS. We define the channel from the j^{th} BS to the RIS as $\boldsymbol{G}_j \in \mathbb{C}^{N\times M}$ and the channel from the RIS to the k^{th} user in the j^{th} cell as $\boldsymbol{h}_{j,k} \in \mathbb{C}^{N\times 1}, \forall j \in \mathcal{J}, k \in \mathcal{K}$. Each user suffers from inter-cell and intra-cell interference simultaneously. Therefore, the received signal of the k^{th} user in the j^{th} cell can be expressed as

$$\begin{aligned} y_{j,k} =& \boldsymbol{h}_{j,k}^{\mathrm{H}}\boldsymbol{\Phi}\boldsymbol{G}_j\boldsymbol{w}_{j,k}s_{j,k} \\ &+ \underbrace{\sum_{l=1,l\neq k}^{K}\boldsymbol{h}_{j,k}^{\mathrm{H}}\boldsymbol{\Phi}\boldsymbol{G}_j\boldsymbol{w}_{j,l}s_{j,l}}_{\text{intra-cell interference}} \\ &+ \underbrace{\sum_{q=1,q\neq j}^{J}\sum_{l=1}^{K}\boldsymbol{h}_{j,k}^{\mathrm{H}}\boldsymbol{\Phi}\boldsymbol{G}_q\boldsymbol{w}_{q,l}s_{q,l}}_{\text{inter-cell interference}} + n_{j,k}, \end{aligned} \tag{1}$$

where $s_{j,k}$ represents the information symbol for the k^{th} user in the j^{th} cell with $\mathbb{E}\left\{|s_{j,k}|^2\right\} = 1$, $\boldsymbol{w}_{j,k} \in \mathbb{C}^{M\times 1}$ represents the transmit beamforming vector from the j^{th} BS to the k^{th} user, $\sum_{k\in\mathcal{K}}\|\boldsymbol{w}_{j,k}\|^2 \leq P_{\max,j}$, $P_{\max,j}$ denotes the maximum power budget of the j^{th} cell, $\boldsymbol{\Phi} = \operatorname{diag}\left(\mathrm{e}^{\mathrm{j}\theta_1}, \mathrm{e}^{\mathrm{j}\theta_2}, \cdots, \mathrm{e}^{\mathrm{j}\theta_N}\right) \in \mathbb{C}^{N\times N}$ denotes the phase shift matrix of RIS, j denotes the imaginary unit, θ_n represents the phase shift of the n^{th} reflecting unit, and $n_{j,k} \sim \mathrm{CN}\left(0, \sigma_{j,k}^2\right)$ represents the noise at the k^{th} user in the j^{th} cell.

For simplicity, let $\boldsymbol{f}_{q,j,k} = \boldsymbol{G}_q^{\mathrm{H}}\boldsymbol{\Phi}^{\mathrm{H}}\boldsymbol{h}_{j,k}$ represent the equivalent channel from the q^{th} BS to the k^{th} user in the j^{th} cell. Then, Eq. (1) can be simplified to

$$\begin{aligned} y_{j,k} =& \boldsymbol{f}_{j,j,k}^{\mathrm{H}}\boldsymbol{w}_{j,k}s_{j,k} + \sum_{l=1,l\neq k}^{K}\boldsymbol{f}_{j,j,k}^{\mathrm{H}}\boldsymbol{w}_{j,l}s_{j,l} \\ &+ \sum_{q=1,q\neq j}^{J}\sum_{l=1}^{K}\boldsymbol{f}_{q,j,k}^{\mathrm{H}}\boldsymbol{w}_{q,l}s_{q,l} + n_{j,k}. \end{aligned} \tag{2}$$

It follows from Eq. (2) that the signal-to-interference plus noise ratio (SINR) of the k^{th} user in the j^{th} cell is

$$\gamma_{j,k} = \frac{\left|\boldsymbol{f}_{j,j,k}^{\mathrm{H}}\boldsymbol{w}_{j,k}\right|^2}{\sum\sum_{(q,l)\neq(j,k)}\left|\boldsymbol{f}_{q,j,k}^{\mathrm{H}}\boldsymbol{w}_{q,l}\right|^2 + \sigma_{j,k}^2}. \tag{3}$$

The achievable rate of the k^{th} user in the j^{th} cell is given by

$$R_{j,k} = \log_2\left(1+\gamma_{j,k}\right), \tag{4}$$

and the achievable sum rate of the considered system is obtained by

$$R = \sum_{j=1}^{J}\sum_{k=1}^{K}R_{j,k}. \tag{5}$$

2.2 Total power consumption model

According to Wang JH et al. (2022), the total power consumption of RIS with discrete phase shift can be modeled as

$$P_{\text{RIS}} = P_{\text{static}} + P_{\text{dynamic}}, \tag{6}$$

where P_{static} and P_{dynamic} represent the static power consumption generated by the control circuit and the dynamic power consumption generated by the RIS reflecting units, respectively.

For the kind of RIS implemented by PIN diodes, its dynamic power consumption is not only affected by the bit resolution of the reflecting unit but also related to the coding status. When the phase shift resolution of each reflecting unit is B-bit, the set of possible discrete phase shifts of each reflecting unit is

$$\theta_n \in \mathcal{F} \triangleq \frac{2\pi m}{2^B}, m \in [0, 2^B-1], m \in \mathbb{Z},\ \forall n. \tag{7}$$

Each quantified phase shift value in the set $\mathcal{F}$ has a unique B-bit encoding pattern. Let us denote the encoding pattern of θ_n in binary as β_n. The RIS

phase shift coding for $B = 1, 2$, and 3 are listed in Table 1.

Table 1 RIS phase shift coding

B-bit	θ_n	β_n
1-bit	0	0
	π	1
2-bit	0	00
	$\pi/2$	01
	π	11
	$3\pi/2$	10
3-bit	0	000
	$\pi/4$	001
	$\pi/2$	011
	$3\pi/4$	010
	π	110
	$5\pi/4$	111
	$3\pi/2$	101
	$7\pi/4$	100

The dynamic power consumption of a RIS implemented by PIN diodes can be written as

$$P_{\text{dynamic}} = \sum_{n=1}^{N} b_n\left(\beta_n\right) \cdot P_{\text{PIN}}, \tag{8}$$

where $b_n\left(\beta_n\right)$ represents the number of bits encoded as "1" in β_n, and P_{PIN} is the power consumption of a PIN transistor when it is encoded as "1." Taking 2-bit resolution phase shift as an example, $b_n(\beta_n) = 2$ when $\beta_n = 11$, $b_n(\beta_n) = 1$ when $\beta_n = 10$ or 01, and $b_n(\beta_n) = 0$ when $\beta_n = 00$. Note that we will consider the RIS with 1-bit phase shift resolution in the rest of the paper.

The total power consumption of the system, including the transmission power of each BS, the circuit power consumption of each BS and user, and the total power consumption of the RIS, is then given by (Huang CW et al., 2019)

$$P_{\text{total}} = \nu^{-1} \sum_{j=1}^{J} \sum_{k=1}^{K} \left\|\boldsymbol{w}_{j,k}\right\|^2 + P_{\text{RIS}} + P_{\text{const}}, \tag{9}$$

where ν is the efficiency of the transmit power amplifier, $P_{\text{const}} = J\left(P_{\text{BS}} + K P_{\text{user}}\right)$, and P_{BS} and P_{user} represent the static circuit power dissipated at each BS and user, respectively.

3 Energy efficiency optimization

3.1 Problem formulation

With the total power consumption and achievable sum rate mentioned in the previous section, the energy efficiency of the considered system is obtained by $\delta = R/P_{\text{total}}$, which is further written as

$$\delta = \frac{\sum\limits_{j=1}^{J} \sum\limits_{k=1}^{K} \log_2\left(1 + \gamma_{j,k}\right)}{\nu^{-1} \sum\limits_{j=1}^{J} \sum\limits_{k=1}^{K} \left\|\boldsymbol{w}_{j,k}\right\|^2 + P_{\text{RIS}} + P_{\text{const}}}. \tag{10}$$

In this section, we aim to jointly optimize the transmit beamforming vectors at each BS and the RIS phase shift matrix to maximize the energy efficiency of the system. At the same time, each user should satisfy the quality-of-service (QoS) constraint. Then, the optimization problem can be formulated as

$$\begin{aligned} &\max_{\boldsymbol{w}_{j,k}, \boldsymbol{\theta}} \ \delta \\ &\text{s.t.} \ \sum_{k=1}^{K} \left\|\boldsymbol{w}_{j,k}\right\|^2 \leq P_{\max,j}, \ \forall j, \\ &\quad R_{j,k} \geq R_{\min,j,k}, \ \forall j, k, \\ &\quad \theta_n \in \mathcal{F}, \ \forall n = 1, 2, \cdots, N, \end{aligned} \tag{11}$$

where $\boldsymbol{\theta} = [\theta_1, \theta_2, \cdots, \theta_N]^{\mathrm{T}}$ is the RIS phase shift vector and $R_{\min,j,k}$ represents the QoS constraint of the k^{th} user in the j^{th} cell.

Problem (11) is a non-convex problem due to the RIS discrete phase shift constraints, and the coupling of the transmit beamforming vectors at the BS and RIS phase shift matrix makes it intractable. To solve the above problem, we propose an alternative optimization architecture to decompose the transmit beamforming vectors at the BS and the RIS phase shift matrix.

The objective function of the above optimization problem, i.e., δ, is in fractional form, and is difficult to solve. First, we need to transform it into a more solvable form by introducing an auxiliary variable λ (Zeng et al., 2021). Problem (11) is

transformed into

$$\begin{aligned}\max_{\boldsymbol{w}_{j,k},\boldsymbol{\theta},\lambda}\ & \sum_{j=1}^{J}\sum_{k=1}^{K}\log_2\left(1+\gamma_{j,k}\right)-\lambda P_{\text{total}}\\ \text{s.t.}\ & \sum_{k=1}^{K}\left\|\boldsymbol{w}_{j,k}\right\|^2\le P_{\max,j},\ \forall j,\\ & R_{j,k}\ge R_{\min,j,k},\ \forall j,k,\\ & \theta_n\in\mathcal{F},\ \forall n=1,2,\cdots,N.\end{aligned}\tag{12}$$

The optimal solution of λ is given by

$$\lambda^{\text{opt}}=\frac{1}{P_{\text{total}}}\sum_{j=1}^{J}\sum_{k=1}^{K}\log_2\left(1+\gamma_{j,k}\right).\tag{13}$$

In this case, problem (12) is equivalent to the original problem (11). Then we investigate the optimization of $\boldsymbol{w}_{j,k}$ and $\boldsymbol{\theta}$ under fixed λ. Introducing the Lagrangian multiplier $\rho_{j,k}$, we transform the optimization problem into

$$\begin{aligned}\max_{\boldsymbol{w}_{j,k},\boldsymbol{\theta}}\ & \sum_{j=1}^{J}\sum_{k=1}^{K}\left(1+\rho_{j,k}\right)R_{j,k}-\lambda P_{\text{total}}\\ \text{s.t.}\ & \sum_{k=1}^{K}\left\|\boldsymbol{w}_{j,k}\right\|^2\le P_{\max,j},\ \forall j,\\ & \theta_n\in\mathcal{F},\ \forall n=1,2,\cdots,N,\end{aligned}\tag{14}$$

where $\boldsymbol{\rho}=[\rho_{1,1},\cdots,\rho_{J,K}]^{\mathrm{T}}$, with $\rho_{j,k}\ge 0$ ($j=1,2,\cdots,J$, $k=1,2,\cdots,K$) being the Lagrangian multiplier chosen to satisfy the QoS contraint $R_{j,k}\ge R_{\min,j,k},\forall j,k$.

Let us define the mean square error (MSE) of the k^{th} user in the j^{th} cell under the receive filter $r_{j,k}$ as

$$E_{j,k}=\mathbb{E}\left\{\left|\hat{s}_{j,k}-s_{j,k}\right|^2\right\},\tag{15}$$

where $\hat{s}_{j,k}=r_{j,k}^{*}y_{j,k}$. Substituting $\hat{s}_{j,k}$ into Eq. (15), we have

$$\begin{aligned}E_{j,k}=&\sum_{q=1}^{J}\sum_{l=1}^{K}\left|r_{j,k}\right|^2\boldsymbol{f}_{q,j,k}^{\mathrm{H}}\boldsymbol{w}_{q,l}\boldsymbol{w}_{q,l}^{\mathrm{H}}\boldsymbol{f}_{q,j,k}\\ &-r_{j,k}^{*}\boldsymbol{f}_{j,j,k}^{\mathrm{H}}\boldsymbol{w}_{j,k}-\boldsymbol{w}_{j,k}^{\mathrm{H}}\boldsymbol{f}_{j,j,k}r_{j,k}\\ &+\left|r_{j,k}\right|^2\sigma_{j,k}^2+1.\end{aligned}\tag{16}$$

Next, introducing an additional auxiliary variable $\chi_{j,k}$, problem (14) is equivalent to (Christensen et al., 2008)

$$\begin{aligned}\min_{\boldsymbol{w}_{j,k},\boldsymbol{\theta},\chi_{j,k},r_{j,k}}\ & g(\boldsymbol{w}_{j,k},\boldsymbol{\theta},\chi_{j,k},r_{j,k})\\ \text{s.t.}\ & \sum_{k=1}^{K}\left\|\boldsymbol{w}_{j,k}\right\|^2\le P_{\max,j},\ \forall j,\\ & \theta_n\in\mathcal{F},\ \forall n=1,2,\cdots,N.\end{aligned}\tag{17}$$

The definition of $g(\boldsymbol{w}_{j,k},\boldsymbol{\theta},\chi_{j,k},r_{j,k})$ is shown as

$$\begin{aligned}&g(\boldsymbol{w}_{j,k},\boldsymbol{\theta},\chi_{j,k},r_{j,k})\\ &=\sum_{j=1}^{J}\sum_{k=1}^{K}\left[\chi_{j,k}E_{j,k}-\left(1+\rho_{j,k}\right)\ln\left(\left(1+\rho_{j,k}\right)^{-1}\chi_{j,k}\right)\right]\\ &\quad+\lambda P_{\text{total}}.\end{aligned}\tag{18}$$

Next, we propose an alternative optimization algorithm to solve the transformed problem (17).

3.2 Transmit beamforming optimization

With the given phase shift matrix $\boldsymbol{\Phi}$, let us consider the optimization of the transmit beamforming vectors. In this case, the optimization problem (17) can be reduced to

$$\begin{aligned}\min_{\boldsymbol{w}_{j,k},\chi_{j,k},r_{j,k}}\ & g(\boldsymbol{w}_{j,k}\boldsymbol{\theta},\chi_{j,k},r_{j,k})\\ \text{s.t.}\ & \sum_{k=1}^{K}\left\|\boldsymbol{w}_{j,k}\right\|^2\le P_{\max,j},\forall j.\end{aligned}\tag{19}$$

To solve problem (19), we also use an alternative optimization method. First, optimize $\chi_{j,k}$ with the other parameters fixed. Let the first-order derivative of $g(\boldsymbol{w}_{j,k},\boldsymbol{\theta},\chi_{j,k},r_{j,k})$ with respect to $\chi_{j,k}$ equal zero; we can obtain the optimal $\chi_{j,k}$ as

$$\chi_{j,k}^{\text{opt}}=\left(1+\rho_{j,k}\right)E_{j,k}^{-1}.\tag{20}$$

When optimizing $r_{j,k}$ with other parameters fixed, the objective function of problem (19) can be simplified to $\min\limits_{r_{j,k}}\sum\limits_{j=1}^{J}\sum\limits_{k=1}^{K}\chi_{j,k}E_{j,k}$. It can be further decoupled into JK sub-problems, i.e., $\min\limits_{r_{j,k}}\chi_{j,k}E_{j,k},\forall j,k$. By setting the first-order derivative of these simplified objective functions to zero, we can obtain the optimal $r_{j,k}$ as

$$r_{j,k}^{\text{opt}}=\varpi^{-1}\boldsymbol{f}_{j,j,k}^{\mathrm{H}}\boldsymbol{w}_{j,k},\tag{21}$$

where

$$\varpi=\sum_{q=1}^{J}\sum_{l=1}^{K}\left(\boldsymbol{f}_{q,j,k}^{\mathrm{H}}\boldsymbol{w}_{q,l}\boldsymbol{w}_{q,l}^{\mathrm{H}}\boldsymbol{f}_{q,j,k}\right)+\sigma_{j,k}^2.\tag{22}$$

With fixed $r_{j,k}$ and $\chi_{j,k}$, problem (19) is simplified to

$$\min_{\boldsymbol{w}_{j,k}} \sum_{j=1}^{J}\sum_{k=1}^{K}(\chi_{j,k}E_{j,k})+\left(\lambda\nu^{-1}+\eta_j\right)\sum_{j=1}^{J}\sum_{k=1}^{K}\|\boldsymbol{w}_{j,k}\|^2, \tag{23}$$

where $\boldsymbol{\eta}=[\eta_1,\eta_2,\cdots,\eta_J]^{\mathrm{T}}$ ($\eta_j>0$, $j=[1,2,\cdots,J]$) is the Lagrangian multiplier related to the transmit power constraint of the j^{th} BS.

Substituting Eq. (16) into the objective function of problem (23), and after some manipulation, problem (23) is decoupled into the following J independent sub-problems:

$$\begin{aligned}&\min_{\boldsymbol{w}_{j,k}}\ \mathcal{L}_j\left(\boldsymbol{w}_{j,k}\right)\\&=\sum_{k=1}^{K}\left(\sum_{q=1}^{J}\sum_{l=1}^{K}\chi_{q,l}|r_{q,l}|^2\boldsymbol{w}_{j,k}^{\mathrm{H}}\boldsymbol{f}_{j,q,l}\boldsymbol{f}_{j,q,l}^{\mathrm{H}}\boldsymbol{w}_{j,k}\right)\\&\quad-\sum_{k=1}^{K}\left(\chi_{j,k}r_{j,k}^{*}\boldsymbol{f}_{j,j,k}^{\mathrm{H}}\boldsymbol{w}_{j,k}\right)\\&\quad-\sum_{k=1}^{K}\left(\chi_{j,k}r_{j,k}\boldsymbol{w}_{j,k}^{\mathrm{H}}\boldsymbol{f}_{j,j,k}\right)\\&\quad+\left(\lambda\nu^{-1}+\eta_j\right)\sum_{k=1}^{K}\|\boldsymbol{w}_{j,k}\|^2,\ \forall j.\end{aligned} \tag{24}$$

Then, letting $\partial\mathcal{L}_j\left(\boldsymbol{w}_{j,k}\right)/\partial\boldsymbol{w}_{j,k}=0$, we obtain the optimal solution of the transmit beamforming vector $\boldsymbol{w}_{j,k}$:

$$\boldsymbol{w}_{j,k}^{\mathrm{opt}}=\chi_{j,k}r_{j,k}\boldsymbol{\Pi}^{-1}\boldsymbol{f}_{j,j,k}, \tag{25}$$

where

$$\boldsymbol{\Pi}=\sum_{q=1}^{J}\sum_{l=1}^{K}\chi_{q,l}|r_{q,l}|^2\boldsymbol{f}_{j,q,l}\boldsymbol{f}_{j,q,l}^{\mathrm{H}}+\left(\lambda\nu^{-1}+\eta_j\right)\boldsymbol{I}_M. \tag{26}$$

Finally, we use the bisection method to obtain the Lagrangian multipliers $\boldsymbol{\eta}$ and $\boldsymbol{\rho}$ (Pan et al., 2020).

3.3 Phase shift matrix optimization

In this subsection, we optimize the RIS phase shift matrix. With all the other parameters fixed, problem (17) can be rewritten as

$$\begin{aligned}&\min_{\boldsymbol{\theta}}\ y\left(\boldsymbol{\theta}\right)+\lambda P_{\mathrm{dynamic}}\\&\text{s.t. }\theta_n\in\mathcal{F},\ \forall n=1,2,\cdots,N.\end{aligned} \tag{27}$$

The expression of $y\left(\boldsymbol{\theta}\right)$ is given as

$$\begin{aligned}&y\left(\boldsymbol{\theta}\right)\\&=\sum_{j=1}^{J}\sum_{k=1}^{K}\chi_{j,k}\Bigg(\sum_{q=1}^{J}\sum_{l=1}^{K}|r_{j,k}|^2\boldsymbol{f}_{q,j,k}^{\mathrm{H}}\boldsymbol{w}_{q,l}\boldsymbol{w}_{q,l}^{\mathrm{H}}\boldsymbol{f}_{q,j,k}\\&\quad-r_{j,k}^{*}\boldsymbol{f}_{j,j,k}^{\mathrm{H}}\boldsymbol{w}_{j,k}-\boldsymbol{w}_{q,l}^{\mathrm{H}}\boldsymbol{f}_{q,j,k}r_{j,k}\Bigg).\end{aligned} \tag{28}$$

Let us define

$$\boldsymbol{Y}_{j,k}=\chi_{j,k}|r_{j,k}|^2\boldsymbol{h}_{j,k}\boldsymbol{h}_{j,k}^{\mathrm{H}}, \tag{29}$$

$$\boldsymbol{Y}=\sum_{j=1}^{J}\sum_{k=1}^{K}\boldsymbol{Y}_{j,k}, \tag{30}$$

$$\boldsymbol{Z}=\sum_{q=1}^{J}\sum_{l=1}^{K}\boldsymbol{G}_q\boldsymbol{w}_{q,l}\boldsymbol{w}_{q,l}^{\mathrm{H}}\boldsymbol{G}_q^{\mathrm{H}}, \tag{31}$$

$$\boldsymbol{Q}_{j,k}=\chi_{j,k}r_{j,k}^{*}\boldsymbol{G}_j\boldsymbol{w}_{j,k}\boldsymbol{h}_{j,k}^{\mathrm{H}}, \tag{32}$$

$$\boldsymbol{Q}=\sum_{j=1}^{J}\sum_{k=1}^{K}\boldsymbol{Q}_{j,k}. \tag{33}$$

Then, $y\left(\boldsymbol{\theta}\right)$ can be converted to

$$y(\boldsymbol{\theta})=\mathrm{tr}\left(\boldsymbol{\Phi}^{\mathrm{H}}\boldsymbol{Y}\boldsymbol{\Phi}\boldsymbol{Z}\right)-\mathrm{tr}\left(\boldsymbol{\Phi}\boldsymbol{Q}\right)-\mathrm{tr}\left(\boldsymbol{\Phi}^{\mathrm{H}}\boldsymbol{Q}^{\mathrm{H}}\right). \tag{34}$$

According to the matrix transformation, we can obtain

$$\mathrm{tr}\left(\boldsymbol{\Phi}^{\mathrm{H}}\boldsymbol{Y}\boldsymbol{\Phi}\boldsymbol{Z}\right)=\boldsymbol{\varphi}^{\mathrm{H}}\left(\boldsymbol{Y}\odot\boldsymbol{Z}^{\mathrm{T}}\right)\boldsymbol{\varphi}, \tag{35}$$

$$\mathrm{tr}\left(\boldsymbol{\Phi}\boldsymbol{Q}\right)=\boldsymbol{\varphi}^{\mathrm{T}}\boldsymbol{q}, \tag{36}$$

where $\boldsymbol{\varphi}=\left[\mathrm{e}^{\mathrm{j}\theta_1},\mathrm{e}^{\mathrm{j}\theta_2},\cdots,\mathrm{e}^{\mathrm{j}\theta_N}\right]^{\mathrm{T}}$ represents the RIS phase shift vector, and $\boldsymbol{q}=\left[[\boldsymbol{Q}]_{1,1},\cdots,[\boldsymbol{Q}]_{N,N}\right]^{\mathrm{T}}$ is a vector composed of diagonal elements of $\boldsymbol{Q}$. Then Eq. (34) can be further simplified to

$$y(\boldsymbol{\theta})=\boldsymbol{\varphi}^{\mathrm{H}}\left(\boldsymbol{Y}\odot\boldsymbol{Z}^{\mathrm{T}}\right)\boldsymbol{\varphi}-2\mathrm{Re}\left\{\boldsymbol{\varphi}^{\mathrm{H}}\boldsymbol{q}^{*}\right\}. \tag{37}$$

Note that the problem is still very difficult to solve, due to the discrete relationship between the power consumption of the RIS reflecting units and its phase shift, as well as the discrete phase shift itself. To solve this problem, we consider extending the discrete phase shift into a continuous phase shift, and then construct a continuous function to approximate the relationship between the continuous phase shift and dynamic power consumption.

Because $b_n(\beta_n)=0$ when $\theta_n=0$ and $b_n(\beta_n)=1$ when $\theta_n=\pi$, we construct the following function

to approximate the relationship between $b_n(\beta_n)$ and θ_n:

$$b_n\left(\beta_n\right)=-\frac{1}{2}\cos\theta_n+\frac{1}{2}. \tag{38}$$

To illustrate the relationship in Eq. (38) more intuitively, graphical representation is used for clear demonstration, as shown in Fig. 2.

Then, substituting Eq. (38) into Eq. (8), we can obtain

$$\begin{aligned}P_{\text{dynamic}}&=\sum_{n=1}^{N}P_{\text{PIN}}\left(-\frac{1}{2}\cos\theta_n+\frac{1}{2}\right)\\&=-\frac{1}{2}P_{\text{PIN}}\left(\text{Re}\left\{\boldsymbol{\varphi}^{\text{H}}\mathbf{1}_{N\times1}\right\}-N\right).\end{aligned} \tag{39}$$

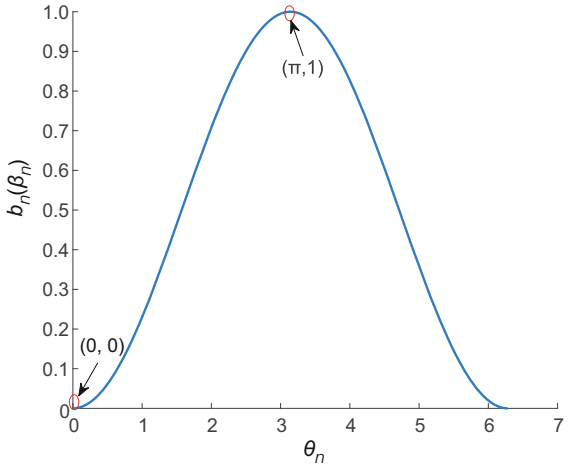

Fig. 2 $b_n(\beta_n)$ versus θ_n

Combining Eqs. (37) and (39), and relaxing the discrete constraint of θ_n, optimization problem (17) is transformed into

$$\begin{aligned}\min_{\boldsymbol{\varphi}}\ &\left(\boldsymbol{\varphi}^{\text{H}}\left(\boldsymbol{Y}\odot\boldsymbol{Z}^{\text{T}}\right)\boldsymbol{\varphi}-2\text{Re}\left\{\boldsymbol{\varphi}^{\text{H}}\boldsymbol{q}^{*}\right\}\right.\\&\left.-\frac{1}{2}\lambda P_{\text{PIN}}\text{Re}\left\{\boldsymbol{\varphi}^{\text{H}}\mathbf{1}_{N\times1}\right\}\right)\\\text{s.t. }&\theta_n\in[0,2\pi),\ \forall n=1,2,\cdots,N.\end{aligned} \tag{40}$$

Subsequently, we apply the MM algorithm to deal with the above non-convex optimization problem. The value of the objective function after the t^{th} iteration is denoted as $f\left(\boldsymbol{\varphi}^t\right)$. Then, at the $(t+1)^{\text{th}}$ iteration, we need to introduce a more tractable upper bound $u\left(\boldsymbol{\varphi},\boldsymbol{\varphi}^t\right)$ of the objective function to replace the original one. However, the upper bound $u\left(\boldsymbol{\varphi},\boldsymbol{\varphi}^t\right)$ should satisfy the following conditions: (1) $u\left(\boldsymbol{\varphi}^t,\boldsymbol{\varphi}^t\right)=f\left(\boldsymbol{\varphi}^t\right)$, (2) $\nabla_{\boldsymbol{\varphi}}u\left(\boldsymbol{\varphi},\boldsymbol{\varphi}^t\right)|_{\boldsymbol{\varphi}=\boldsymbol{\varphi}^t}=\nabla_{\boldsymbol{\varphi}}f\left(\boldsymbol{\varphi}^t\right)|_{\boldsymbol{\varphi}=\boldsymbol{\varphi}^t}$, and (3) $u\left(\boldsymbol{\varphi},\boldsymbol{\varphi}^t\right)\geq f\left(\boldsymbol{\varphi}\right)$. Only when the above conditions are met, will the results obtained in each iteration make the objective function gradually decrease until convergence.

According to Sun et al. (2017), for any $\boldsymbol{\varphi}$, we have the following upper bound of the objective function:

$$\begin{aligned}&\boldsymbol{\varphi}^{\text{H}}\left(\boldsymbol{Y}\odot\boldsymbol{Z}^{\text{T}}\right)\boldsymbol{\varphi}\\&\leq\boldsymbol{\varphi}^{\text{H}}\boldsymbol{W}\boldsymbol{\varphi}-2\text{Re}\left\{\boldsymbol{\varphi}^{\text{H}}\left(\boldsymbol{W}-\boldsymbol{Y}\odot\boldsymbol{Z}^{\text{T}}\right)\boldsymbol{\varphi}^t\right\}\\&+\left(\boldsymbol{\varphi}^t\right)^{\text{H}}\left(\boldsymbol{W}-\boldsymbol{Y}\odot\boldsymbol{Z}^{\text{T}}\right)\boldsymbol{\varphi}^t=u_1\left(\boldsymbol{\varphi},\boldsymbol{\varphi}^t\right),\end{aligned} \tag{41}$$

where $\boldsymbol{W}=\varsigma_{\max}\boldsymbol{I}_N$, and $\varsigma_{\max}$ is the maximum eigenvalue of $\boldsymbol{Y}\odot\boldsymbol{Z}^{\text{T}}$. Thus, we change the objective function of problem (40) into the following one:

$$\begin{aligned}u\left(\boldsymbol{\varphi},\boldsymbol{\varphi}^t\right)=&u_1\left(\boldsymbol{\varphi},\boldsymbol{\varphi}^t\right)-2\text{Re}\left\{\boldsymbol{\varphi}^{\text{H}}\boldsymbol{q}^{*}\right\}\\&-\frac{1}{2}\lambda P_{\text{PIN}}\text{Re}\left\{\boldsymbol{\varphi}^{\text{H}}\mathbf{1}_{N\times1}\right\}.\end{aligned} \tag{42}$$

Note that $\boldsymbol{\varphi}^{\text{H}}\boldsymbol{W}\boldsymbol{\varphi}=\varsigma_{\max}N$ is a constant. After removing all constants, we have the following optimization problem:

$$\begin{aligned}\max_{\boldsymbol{\varphi}}\ &2\text{Re}\left\{\boldsymbol{\varphi}^{\text{H}}\boldsymbol{x}\right\}\\\text{s.t. }&\theta_n\in[0,2\pi),\ \forall n=1,2,\cdots,N,\end{aligned} \tag{43}$$

where $\boldsymbol{x}=\left(\boldsymbol{W}-\boldsymbol{Y}\odot\boldsymbol{Z}^{\text{T}}\right)\boldsymbol{\varphi}^t+\boldsymbol{q}^{*}+\frac{1}{4}\lambda P_{\text{PIN}}\mathbf{1}_{N\times1}$. Therefore, the optimal solution can be directly obtained as follows:

$$\boldsymbol{\varphi}^{\text{opt}}=\text{e}^{\text{j}\arg(\boldsymbol{x})}. \tag{44}$$

Finally, we discretize $\boldsymbol{\varphi}^{\text{opt}}$ into the nearest phase shift in $\mathcal{F}$.

3.4 Algorithm summary

The proposed overall algorithm is given in Algorithm 1. At each step of the proposed algorithm, the objective function is ensured to be non-decreasing, which can be proved by the following inequality:

$$\begin{aligned}\delta\left(\boldsymbol{w}_{j,k}^{(r)},\boldsymbol{\Phi}^{(r)}\right)&\leq\delta\left(\boldsymbol{w}_{j,k}^{(r+1)},\boldsymbol{\Phi}^{(r)}\right)\\&\leq\delta\left(\boldsymbol{w}_{j,k}^{(r+1)},\boldsymbol{\Phi}^{(r+1)}\right),\end{aligned} \tag{45}$$

where $(\cdot)^{(r)}$ represents the r^{th} iteration.

The objective function has an upper bound due to the limitation of the transmit power at each BS, so Algorithm 1 is guaranteed to converge to at least a local optimal solution of problem (11).

Subsequently, the complexity of the overall algorithm is analyzed. The complexity of calculating the transmit beamforming vector $\boldsymbol{w}_{j,k}$ is $O\left(JKM^3\right)$. The complexity of updating the RIS phase shift vector $\boldsymbol{\varphi}$ is $O\left(N^3+I_{\mathrm{t}}N^2\right)$, where I_{t} denotes the iteration number for optimizing the RIS phase shift. Therefore, the overall complexity of the proposed Algorithm 1 is $O\left(\max\left\{O\left(JKM^3\right),O\left(N^3+I_{\mathrm{t}}N^2\right)\right\}\right)$.

Algorithm 1 Proposed algorithm for solving problem (11)

Initialize the threshold ζ, the iteration number $r=0$, $\boldsymbol{\Phi}^{(0)}$, $\boldsymbol{w}_{j,k}^{(0)}=\mathbf{1}_{M\times 1}$
repeat
  Set $r=r+1$
  Calculate $r_{j,k}^{(r)}$ via Eq. (21)
  Calculate $\chi_{j,k}^{(r)}$ via Eq. (20)
  Calculate $\lambda^{(r)}$ via Eq. (13)
  Calculate $\boldsymbol{w}_{j,k}^{(r)}$ via Eq. (25)
  Initialize the threshold ξ and the iteration number $t=0$
  repeat
    Set $t=t+1$
    Calculate $\boldsymbol{\varphi}^{(t)}$ via Eq. (44)
  until $\left|\left(f\left(\boldsymbol{\varphi}^{(t)}\right)-f\left(\boldsymbol{\varphi}^{(t-1)}\right)\right)/f\left(\boldsymbol{\varphi}^{(t-1)}\right)\right|\leq\xi$
  Discretize $\boldsymbol{\varphi}^{(t)}$
  Update $\boldsymbol{\Phi}^{(r)}=\mathrm{diag}\left(\boldsymbol{\varphi}^{(t)}\right)$
until the objective function of problem (11) converges

4 Simulation results

In this section, we provide simulation results to validate the performance of the proposed algorithm for the RIS-assisted multi-cell communication system. The considered system has two cells, each of which is deployed with a BS of eight antennas, and each cell has two users. A RIS with 8×8 reflecting units is deployed at the edge of the two cells. The distance between each BS and the RIS is d_{BI} =100 m, and the distance between each user and the RIS is $d_{\mathrm{IU}}=15$ m. The channel from the j^{th} BS to the RIS is modeled as

$$\boldsymbol{G}_j=\sqrt{\beta(d_{\mathrm{BI}})}\left(\sqrt{\frac{\kappa_j}{1+\kappa_j}}\bar{\boldsymbol{G}}_j+\sqrt{\frac{1}{1+\kappa_j}}\tilde{\boldsymbol{G}}_j\right), \tag{46}$$

and the channel from the RIS to the k^{th} user in the j^{th} cell is modeled as

$$\boldsymbol{h}_{j,k}=\sqrt{\beta(d_{\mathrm{IU}})}\left(\sqrt{\frac{\rho_{j,k}}{\rho_{j,k}+1}}\bar{\boldsymbol{h}}_{j,k}+\sqrt{\frac{1}{\rho_{j,k}+1}}\tilde{\boldsymbol{h}}_{j,k}\right), \tag{47}$$

where $\bar{\boldsymbol{G}}_j$ and $\bar{\boldsymbol{h}}_{j,k}$ represent line-of-sight (LoS) components, $\tilde{\boldsymbol{G}}_j$ and $\tilde{\boldsymbol{h}}_{j,k}$ denote non-LoS (NLoS) components, $\kappa_j=3$ dB and $\rho_{j,k}=6$ dB are Rician factors, $\beta(d)=C_0(d/d_0)^{-\alpha}$ is the large-scale fading coefficient, $C_0=-30$ dB, $d_0=1$ m, α is the path loss factor, and we set 2.6 and 3 for the BS–RIS link and RIS–user link respectively. In addition, we set the noise variance $\sigma_{j,k}^2=-108$ dBm, the transmission bandwidth of 20 MHz, the efficiency of the transmit power amplifier $\nu=1/1.2$, BS circuit power consumption $P_{\mathrm{BS}}=9$ dBW (Le et al., 2021), and user circuit power consumption $P_{\mathrm{user}}=20$ dBm. Note that the relationship between the number of reflecting units and RIS static power consumption can be approximately regarded as linear. In Wang JH et al. (2022), the measured static power consumption of a RIS with 512 reflecting units is 6.52 W. While the number of RIS reflecting units used in this paper is 64, we set the static power consumption to be $6.52/8=0.815$ W in the simulation. Also, we set $P_{\mathrm{s}}=(0.815/N+0.01199)$ W, the power consumption of PIN diode $P_{\mathrm{PIN}}=11.99$ mW, based on the measured value in Wang JH et al. (2022).

In Fig. 3, we set $R_{\min,j,k}=0$; that is, there is no QoS constraint for each user. We compare the performance of the proposed algorithm EEmax with those of three benchmark algorithms, EEmax TRM, SEmax, and random phase shift.

1. EEmax: Based on the practical RIS power consumption model mentioned above, we optimize the communication system using the proposed algorithm in this study to maximize its energy efficiency.

2. EEmax TRM: We use the proposed algorithm to optimize the multi-cell communication system in this study based on the theoretical RIS power consumption model (TRM). The theoretical RIS power consumption is commonly assumed to be a fixed value or even negligible in the majority of existing works. For example, in You L et al. (2021), the RIS power consumption is modeled as

$$P_{\mathrm{RIS}}=NP_{\mathrm{s}}, \tag{48}$$

where P_{s} is assumed to be the static power consumption of each RIS reflecting unit. In the simulation, we

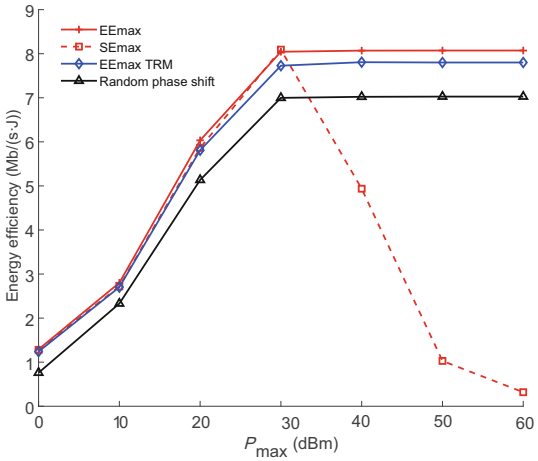

Fig. 3 Energy efficiency versus $P_{\max}$ for our proposed algorithm and three benchmark algorithms

use this theoretical RIS power consumption model for comparison.

3. SEmax: We revise the optimization objective to maximize the spectral efficiency of the system and apply the proposed algorithm in this study for optimization.

4. Random phase shift: The phase shift for each reflecting unit is randomly generated and the transmit beamforming vector of each BS is optimized by our proposed algorithm.

From Fig. 3, it can be seen that the energy efficiency of the EEmax algorithm continues to increase to a certain threshold value with increasing $P_{\max}$. The reason is that when the increase of power consumption brought by the increase in $P_{\max}$ is less than the increase of rate gain, the algorithm will allocate the full power of each BS to do the transmission, until the energy efficiency reaches a maximum value. After that, the increase in transmit power will lead to higher increase of power consumption than that of rate gain. In this case, the algorithm will not allocate the full power for transmission, and the energy efficiency will be maintained at that maximum value. Compared with the random phase shift algorithm, the energy efficiency of the system is significantly improved by using the proposed algorithm.

Comparing the EEmax and SEmax algorithms, it is obvious that the energy efficiency of our proposed algorithm EEmax is better than that of the SEmax algorithm. For $P_{\max} \leq 30$ dBm, the energy efficiency of SEmax is similar to that of EEmax. For $P_{\max} > 30$ dBm, the energy efficiency of SEmax starts to degrade, which is due mainly to the larger power loss caused by the high transmit power.

Furthermore, we compare the theoretical RIS power consumption model with the practical RIS power consumption model. It is observed that the impact of RIS phase shift on RIS power consumption is ignored in the theoretical RIS power consumption model. This leads to an increase in the total power consumption of the system, and thus a decrease in the energy efficiency of the system.

Fig. 4 illustrates the energy efficiency of the system under different numbers of RIS reflecting units N. The other parameters are the same as those in Fig. 3. From Fig. 4, we can see that, as the number of reflecting units increases, the energy efficiency of the system increases. Thus, increasing the number of reflecting units is an effective way of improving the energy efficiency of the system, because the power consumption of each reflecting unit is extremely low.

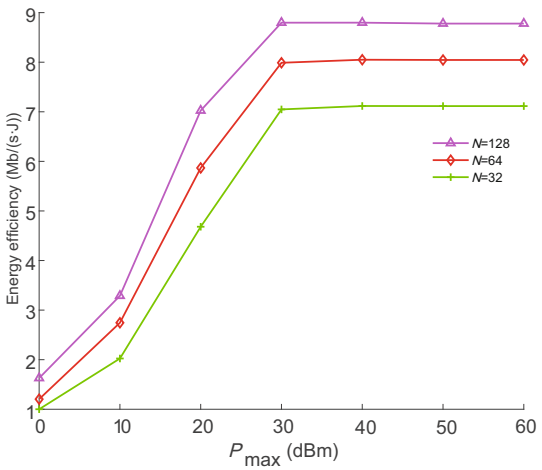

Fig. 4 Energy efficiency with different numbers of RIS reflecting units

Figs. 5 and 6 plot the energy efficiency of the system versus different numbers of users and BS antennas, respectively, in each cell. In Figs. 5 and 6, the other parameters are the same as those in Fig. 3. As can be seen from Fig. 5, the energy efficiency increases with the increase of the number of users. Moreover, with the same transmit power, the energy efficiency of the system is improved by increasing the number of BS antennas.

Fig. 7 shows the energy efficiency with different minimum rates $R_{\min,j,k}$. The simulation results show that the maximum energy efficiency achieved decreases as the QoS constraint $R_{\min,j,k}$ increases.

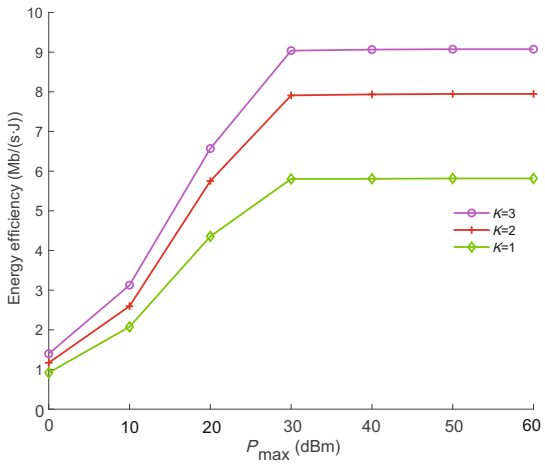

Fig. 5 Energy efficiency with different numbers of users

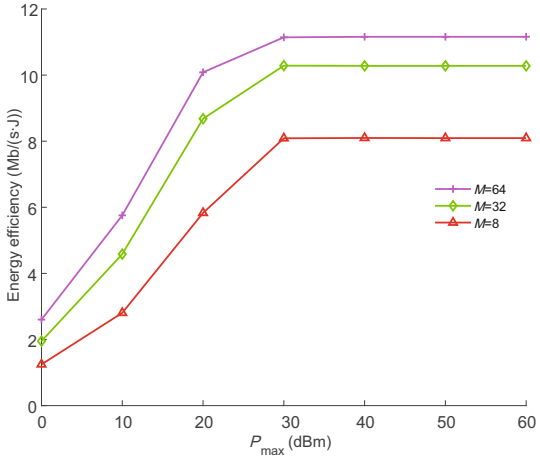

Fig. 6 Energy efficiency with different numbers of BS antennas

This is because, as the user's minimum rate requirement increases, more BS power will be consumed to meet the requirement for users with rough channel conditions. In this case, the increase rate of the system sum rate is lower than that of the system power consumption; thus, the energy efficiency of the system decreases.

5 Conclusions

In this paper, we study a RIS-assisted multi-cell communication system based on a practical RIS power consumption model. Specifically, the problem of maximizing energy efficiency is formulated by jointly optimizing transmit beamforming vectors at each BS and RIS phase shift matrix. We propose an alternative algorithm to solve the non-convex problem. First, we design the transmit beamforming vector based on the converted WMMSE problem. Then, to overcome the inconvenience of the discontinuity relationship between RIS power consumption and discrete phase shift, we establish a continuous alternative function. Subsequently, we use the MM algorithm to optimize the RIS continuous phase shift and finally discretize it. Simulation results reveal that the proposed algorithm has good performance.

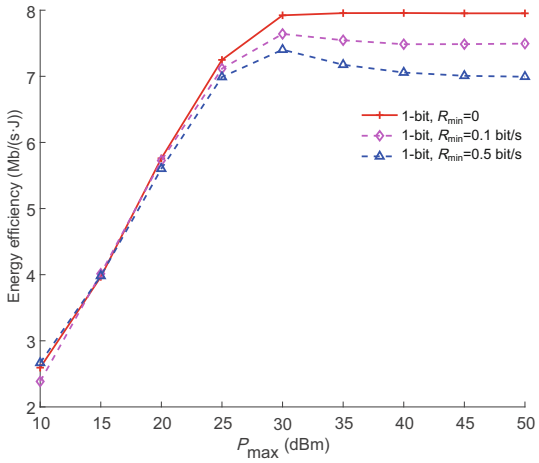

Fig. 7 Energy efficiency with different minimum rates

Contributors

Danning XU and Xiao LI designed the research. Jinghe WANG provided the data. Danning XU drafted the paper. Xiao LI, Yu HAN, and Shi JIN helped organize the paper. Yu HAN, Xiao LI, and Shi JIN revised and finalized the paper.

Compliance with ethics guidelines

Xiao LI is a corresponding expert of *Frontiers of Information Technology & Electronic Engineering*, and Shi JIN is an executive lead editor of this special issue; they were not involved with the peer review process of this paper. All the authors declare that they have no conflict of interest.

Data availability

The data that support the findings of this study are available from the corresponding author upon reasonable request.

References

Chen J, Xie YH, Mu XD, et al., 2022. Energy efficient resource allocation for IRS assisted CoMP systems. *IEEE Trans Wirel Commun*, 21(7):5688-5702. https://doi.org/10.1109/TWC.2022.3142784

Christensen SS, Agarwal R, de Carvalho E, et al., 2008. Weighted sum-rate maximization using weighted MMSE for MIMO-BC beamforming design. *IEEE Trans Wirel Commun*, 7(12):4792-4799. https://doi.org/10.1109/T-WC.2008.070851

Cui TJ, Qi MQ, Wan X, et al., 2014. Coding metamaterials, digital metamaterials and programmable metamaterials. *Light Sci Appl*, 3(10):e218. https://doi.org/10.1038/lsa.2014.99

Cui TJ, Liu S, Zhang L, 2017. Information metamaterials and metasurfaces. *J Mater Chem C*, 5(15):3644-3668. https://doi.org/10.1039/C7TC00548B

di Renzo M, Zappone A, Debbah M, et al., 2020. Smart radio environments empowered by reconfigurable intelligent surfaces: how it works, state of research, and the road ahead. *IEEE J Sel Areas Commun*, 38(11):2450-2525. https://doi.org/10.1109/JSAC.2020.3007211

Feng KM, Wang QS, Li X, et al., 2020. Deep reinforcement learning based intelligent reflecting surface optimization for MISO communication systems. *IEEE Wirel Commun Lett*, 9(5):745-749. https://doi.org/10.1109/LWC.2020.2969167

Feng KM, Li X, Han Y, et al., 2021a. Joint beamforming optimization for reconfigurable intelligent surface-enabled MISO-OFDM systems. *China Commun*, 18(3):63-79. https://doi.org/10.23919/JCC.2021.03.006

Feng KM, Li X, Han Y, et al., 2021b. Physical layer security enhancement exploiting intelligent reflecting surface. *IEEE Commun Lett*, 25(3):734-738. https://doi.org/10.1109/LCOMM.2020.3042344

Gan X, Zhong CJ, Huang CW, et al., 2021. RIS-assisted multi-user MISO communications exploiting statistical CSI. *IEEE Trans Commun*, 69(10):6781-6792. https://doi.org/10.1109/TCOMM.2021.3100860

Gan X, Zhong CJ, Huang CW, et al., 2022. Multiple RISs assisted cell-free networks with two-timescale CSI: performance analysis and system design. *IEEE Trans Commun*, 70(11):7696-7710. https://doi.org/10.1109/TCOMM.2022.3208629

Huang CW, Zappone A, Alexandropoulos GC, et al., 2019. Reconfigurable intelligent surfaces for energy efficiency in wireless communication. *IEEE Trans Wirel Commun*, 18(8):4157-4170. https://doi.org/10.1109/TWC.2019.2922609

Huang CW, Yang ZH, Alexandropoulos GC, et al., 2021. Multi-hop RIS-empowered terahertz communications: a DRL-based hybrid beamforming design. *IEEE J Sel Areas Commun*, 39(6):1663-1677. https://doi.org/10.1109/JSAC.2021.3071836

Huang YW, Mei WD, Zhang R, 2022. Empowering base stations with co-site intelligent reflecting surfaces: user association, channel estimation and reflection optimization. *IEEE Trans Commun*, 70(7):4940-4955. https://doi.org/10.1109/TCOMM.2022.3178762

Jiang LL, Li X, Matthaiou M, et al., 2023. Joint user scheduling and phase shift design for RIS assisted multi-cell MISO systems. *IEEE Wirel Commun Lett*, 12(3):431-435. https://doi.org/10.1109/LWC.2022.3229441

Le QN, Nguyen VD, Dobre OA, et al., 2021. Energy efficiency maximization in RIS-aided cell-free network with limited backhaul. *IEEE Commun Lett*, 25(6):1974-1978. https://doi.org/10.1109/LCOMM.2021.3062275

Liu JX, Xiong K, Lu Y, et al., 2020. Energy efficiency in secure IRS-aided SWIPT. *IEEE Wirel Commun Lett*, 9(11):1884-1888. https://doi.org/10.1109/LWC.2020.3006837

Luo CH, Li X, Jin S, et al., 2021. Reconfigurable intelligent surface-assisted multi-cell MISO communication systems exploiting statistical CSI. *IEEE Wirel Commun Lett*, 10(10):2313-2317. https://doi.org/10.1109/LWC.2021.3100427

Pan CH, Ren H, Wang KZ, et al., 2020. Multicell MIMO communications relying on intelligent reflecting surfaces. *IEEE Trans Wirel Commun*, 19(8):5218-5233. https://doi.org/10.1109/TWC.2020.2990766

Sang J, Yuan YF, Tang WK, et al., 2022. Coverage enhancement by deploying RIS in 5G commercial mobile networks: field trials. *IEEE Wirel Commun*, early access. https://doi.org/10.1109/MWC.011.2200356

Sang J, Zhou MY, Lan JF, et al., 2023. Multi-scenario broadband channel measurement and modeling for sub-6 GHz RIS-assisted wireless communication systems. https://arxiv.org/abs/2305.07835

Sun Y, Babu P, Palomar DP, 2017. Majorization-minimization algorithms in signal processing, communications, and machine learning. *IEEE Trans Signal Process*, 65(3):794-816. https://doi.org/10.1109/TSP.2016.2601299

Tang WK, Li X, Dai JY, et al., 2019. Wireless communications with programmable metasurface: transceiver design and experimental results. *China Commun*, 16(5):46-61. https://doi.org/10.23919/j.cc.2019.05.004

Tang WK, Dai JY, Chen MZ, et al., 2020. MIMO transmission through reconfigurable intelligent surface: system design, analysis, and implementation. *IEEE J Sel Areas Commun*, 38(11):2683-2699. https://doi.org/10.1109/JSAC.2020.3007055

Tang WK, Chen MZ, Chen XY, et al., 2021. Wireless communications with reconfigurable intelligent surface: path loss modeling and experimental measurement. *IEEE Trans Wirel Commun*, 20(1):421-439. https://doi.org/10.1109/TWC.2020.3024887

Wang JH, Tang WK, Liang JC, et al., 2022. Reconfigurable intelligent surface: power consumption modeling and practical measurement validation. https://arxiv.org/abs/2211.00323

Wang TQ, Fang F, Ding ZG, 2022. An SCA and relaxation based energy efficiency optimization for multi-user RIS-assisted NOMA networks. *IEEE Trans Veh Technol*, 71(6):6843-6847. https://doi.org/10.1109/TVT.2022.3162197

You CS, Zheng BX, Zhang R, 2021. Wireless communication via double IRS: channel estimation and passive beamforming designs. *IEEE Wirel Commun Lett*, 10(2):431-435. https://doi.org/10.1109/LWC.2020.3034388

You L, Xiong JY, Huang YF, et al., 2021. Reconfigurable intelligent surfaces-assisted multiuser MIMO uplink transmission with partial CSI. *IEEE Trans Wirel Commun*, 20(9):5613-5627. https://doi.org/10.1109/TWC.2021.3068754

Zeng M, Bedeer E, Dobre OA, et al., 2021. Energy-efficient resource allocation for IRS-assisted multi-antenna uplink systems. *IEEE Wirel Commun Lett*, 10(6):1261-1265. https://doi.org/10.1109/LWC.2021.3063554